Kinetic Deuterium Isotope Effects in the Protonations of $[(\mu\text{-H})M_3(CO)_{11}]^-$ (M = Fe, Ru, Os)

David C. Pribich and Edward Rosenberg*

Department of Chemistry, California State University, Northridge, California 91330

Received November 18, 1987

The rates of low-temperature (−90 to −40 °C) protonation of the anions $[(\mu\text{-H})M_3(CO)_{11}]^-$ (M = Fe, Ru, Os) have been investigated with XSO_3F (X = H or D) in CD_2Cl_2 by using ^1H and ^{13}C NMR techniques. No deuterium kinetic isotope effect is observed on the rate of protonation to give the initially formed oxygen-protonated species $(\mu\text{-H})(COX)M_3(CO)_{10}$ (M = Fe, Ru; X = H or D). However, in the case of ruthenium the rate of transformation of this species to the dihydrido species $(\mu\text{-X})XRu_3(CO)_{11}$ (X = H or D) shows a very large isotope effect (k_H/k_D = 47 at −40 °C). In the case of osmium, the previously unobserved oxygen-deuteriated species $(\mu\text{-H})(COD)Os_3(CO)_{10}$ is seen at −80 °C with DSO_3F. Under these conditions, protonation with HSO_3F yields only $(\mu\text{-H})(H)Os_3(CO)_{11}$. These large isotope effects on ligand to metal hydrogen transfer are discussed in connection with previously observed large isotope effects in cluster protonations.

Introduction

An understanding of the mechanisms and transition states involved in hydrogen transfers from ligands to metal centers (and the reverse processes) in hydrido metal clusters is crucial to the development of these compounds as catalysts and to the general understanding of polymetallic–ligand interactions. Deuterium kinetic isotope effects have long been used in organic chemistry to obtain mechanistic information, and we have been trying to develop a knowledge of the origin of isotope effects observed when deuterium is substituted for hydrogen in hydridometal clusters.[1,2] Mays et. al. observed very large isotope effects in the protonation of neutral and anionic clusters with mineral acids (see Table I).[3] In organic chemistry large isotope effects (i.e. isotope effects larger than calculated values based on differences in zero-point energy) are thought to arise from reactions in which the barrier width is small and where the wavelength of the proton is similar to the width of the barrier. These types of barriers are associated with reactions in which there is very little distortion of the reactant ground-state geometry on going from reactant to product.[4] The most common example of this type of reaction in organic chemistry is intramolecular proton transfer. The presence or absence of large k_H/k_D ratios have been used to characterize the transition states of these proton transfers.[4] In considering the large protonation isotope effects observed by Mays, we thought that their origin might be due to an initial protonation of oxygen followed by an intramolecular proton transfer down to the metal core (eq 1). This seemed to us a very likely

$$[M_n(CO)_m]^{n-} + H^+ \rightarrow [M_n(CO)_{m-1}(COH)]^{1-n} \rightarrow [HM_n(CO)_m]^{1-n} \quad (1)$$

$$n = 0, 1$$

possibility in light of the recent work of Shriver[5] and Kiester[6] on the protonation of $[(\mu\text{-H})M_3(CO)_{11}]^-$ (M = Fe, Ru) (see structure I). Additionally, the recent work of

Table I. Kinetic Isotope Effects in the Protonation of Transition-Metal Clusters[a]

	k_H/k_D
$FeCo_3(CO)_{12}^-$	16.8 ± 1.0
$RuCo_3(CO)_{12}^-$	15.4 ± 1.0
$OsCo_3(CO)_{12}^-$	16.2 ± 1.0
$Os_3(CO)_{12}$	11 ± 2
$[(\pi - C_5H_5)Fe(CO)_2]_2$	7 ± 1

[a] Taken from Knight, J.; Mays, M. J. *J. Chem. Soc. A* **1970**, 711.

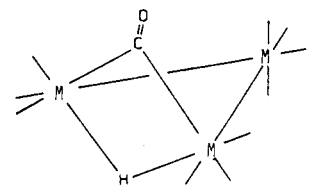

I
M = Fe, Ru, Os

Norton et al. showed that protonation can be kinetically slow but thermodynamically favored at a transition-metal center and can show normal zero-point energy isotope effects for intermolecular self-exchange of protons.[7]

In both the iron[5] and ruthenium[6] cases initial protonation is at oxygen. In the ruthenium case, however, subsequent rearrangement to the dihydride species $(\mu\text{-H})(H)Ru_3(CO)_{11}$ can be observed[6] (eq 2). In this paper a

$$[(\mu\text{-H})Ru_3(\mu\text{-CO})(CO)_{10}]^- + H^+ \xrightarrow{-80\ °C} (\mu\text{-H})Ru_3(\mu\text{-COH})(CO)_{10} \xrightarrow{-80\ °C} (\mu\text{-H})(H)Ru_3(CO)_{11} \quad (2)$$

further investigation of the low-temperature protonation of the $[(\mu\text{-H})M_3(CO)_{11}]^-$ (M = Fe, Ru) anions as well as the first report of the low-temperature protonation of $[(\mu\text{-H})Os_3(CO)_{11}]^-$ is presented. More importantly we report on the observation of very significant deuterium ki-

(1) Rosenberg, E.; Anslyn, E. V.; Barner-Thorsen, C.; Aime, S.; Osella, D.; Gobetto, R.; Milone, L. *Organometallics* **1984**, *3*, 1790.
(2) Barner-Thorsen, C.; Rosenberg, E.; Saatjian, G.; Aime, S.; Milone, L.; Osella, D. *Inorg. Chem.* **1981**, *20*, 1592.
(3) (a) Mays, M. J.; Simpson, R. N. F. *J. Chem. Soc. A* **1968**, 1444. (b) Knight, J.; Mays, M. J. *J. Chem. Soc. A* **1970**, 711.
(4) (a) De La Vega, J. R. *Acc. Chem. Res.* **1982**, *15*, 185. (b) Kwart, H. *Acc. Chem. Res.* **1982**, *15*, 401. (c) Scheiner, S. *Acc. Chem. Res.* **1985**, *18*, 174.
(5) Hodali, H. A.; Shriver, D. F.; Ammlung, C. A. *J. Am. Chem. Soc.* **1978**, *100*, 5239.
(6) Keister, J. B. *J. Organomet. Chem.* **1980**, *190*, C36.
(7) Norton, J. R.; Sullivan, J. M.; Edidin, R. T. *J. Am. Chem. Soc.* **1987**, *109*, 3945.

0276-7333/88/2307-1741$01.50/0

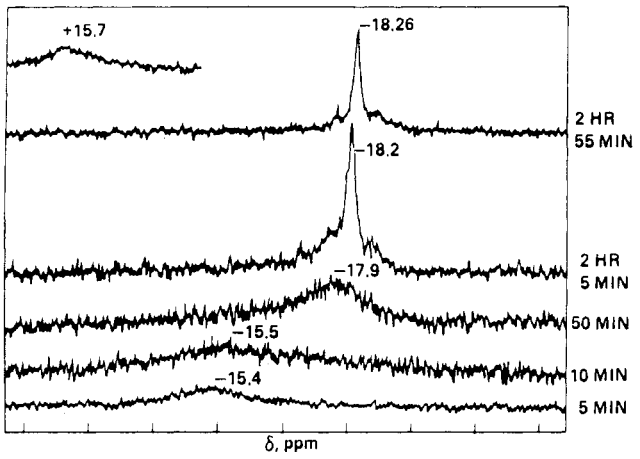

Figure 1. Time-dependent ^1H NMR spectra after addition of 1 equiv of HSO_3F to a CD_2Cl_2 solution of $[PPN][(\mu\text{-}H)Fe_3(CO)_{11}]$ at −80 °C. Original $[(\mu\text{-}H)Fe_3(CO)_{11}]^-$ hydride signal was observed at −15.3 ppm.

netic isotope effects on the transformations presented in eq 2 for the low-temperature protonations of the ruthenium and osmium anions. The mechanistic implications of these isotope effects are discussed.

Results and Discussion

A. Low-Temperature Protonations. 1. $[(\mu\text{-}H)Fe_3(CO)_{11}]^-$. For these studies the compound $[PPN][(\mu\text{-}H)Fe_3(CO)_{11}]$ was used (PPN = $[N(P(C_6H_5)_3)_2]^+$). Care was taken to control the conditions under which acid was added to each of the compounds studied. The cluster anion salt was dissolved in dry CD_2Cl_2 and degassed with nitrogen in an NMR tube. The sample was placed in the precooled NMR probe at −80 °C, and after temperature equilibration, acid was injected below the solution surface by using a long-needled microsyringe. This procedure minimizes the expected temperature increase arising from the heat of mixing of the acid and solvent and was used for all protonation experiments unless otherwise specified.

The $[(\mu\text{-}H)Fe_3(CO)_{11}]^-$ anion with the structure I, shown above, contains one bridging hydride whose ^1H NMR signal appears at −15.3 ppm at −80 °C in CD_2Cl_2. Upon addition of 1 equiv of fluorosulfonic acid (HSO_3F) to 0.5 mL of a 0.068 M CD_2Cl_2 solution of $[PPN][(\mu\text{-}H)Fe_3(CO)_{11}]$ at −80 °C, the time-dependent spectra shown in Figure 1 result. The broad peak that initially appears at −15.4 ppm and moves upfield slowly with time apparently results from proton exchange between anionic and O-protonated cluster at a rate near the fast-exchange limit on the NMR time scale. As more protonated species is formed the peak arrives at −18.2 ppm, sharpens, and does not shift further. This final shift corresponds to that reported by Shriver,[5] with the −18.2 ppm bridging hydride peak and the broad +15.7 ppm peak (Figure 1) representing a proton bound to the oxygen of the bridging carbonyl, i.e., $(\mu\text{-}H)Fe_3(\mu\text{-}COH)(CO)_{10}$. Attempts to simulate the line-shape changes to determine the rate constant for proton exchange or to accurately calculate a second-order rate constant for protonation from the observed changes in chemical shift failed. This is probably because of artificial broadening of the resonances which results from the fact that the time necessary for obtaining the spectrum (2 min) is significant with respect to the rate of protonation. From these data the second-order rate constant for protonation (k_1, eq 3) can be estimated to be

$$[(\mu\text{-}H)Fe_3(CO)_{11}]^- + H^+ \xrightarrow{k_1} (\mu\text{-}H)(\mu\text{-}COH)Fe_3(CO)_{10} \quad (3)$$

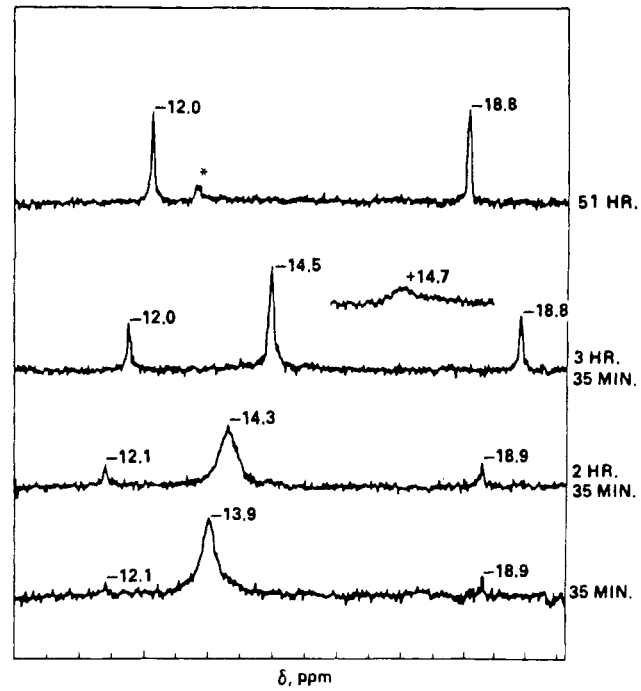

Figure 2. Time-dependent ^1H NMR spectra after addition of 1 equiv of HSO_3F to a CD_2Cl_2 solution of $[(CH_3CH_2)_4N][(\mu\text{-}H)Ru_3(CO)_{11}]$ at −80 °C. Original $(\mu\text{-}H)Ru_3(CO)_{11}^-$ hydride signal (*) was observed at −13.0 ppm, indicating a slight deficiency of acid.

$1.3(\pm 0.3) \times 10^{-3}$ L/(mol·s).[8] Upon warming the species remains unchanged until approximately −30 °C, where decomposition to $Fe_3(CO)_{12}$ and H_2 gas occurred, consistent with the results of Shriver.[5]

2. $[(\mu\text{-}H)Ru_3(CO)_{11}]^-$. The tetraethylammonium salt of the $[(\mu\text{-}H)Ru_3(CO)_{11}]^-$ anion also has structure I and shows the bridging hydride ^1H NMR signal at −13.0 ppm in CD_2Cl_2 at −80 °C. Figure 2 displays the time-dependent ^1H NMR spectra that result from the addition of 1 equiv of HSO_3F to 0.5 mL of a 0.060 M CD_2Cl_2 solution of $[(CH_3CH_2)_4N][(\mu\text{-}H)Ru_3(CO)_{11}]$ at −80 °C. As in the iron case, a broad peak is initially observed which moves slowly upfield until a sharp peak at −14.5 ppm results. However, in this case very small peaks at −12.0 and −18.8 ppm are also observed. These peaks correspond to $(\mu\text{-}H)(H)Ru_3(CO)_{11}$ with both hydrides bound to the metal core, one a terminal hydride (−12.0 ppm) and one a μ-hydride (−18.8 ppm), consistent with the results of Kiester.[6] The −14.5 ppm peak and the broad +14.7 ppm peak correspond to the $(\mu\text{-}H)Ru_3(\mu\text{-}COH)(CO)_{10}$ species,[6] analogous to the iron case. The rate of protonation is the same as for the iron analogue (eq 3). After 51 h at −80 °C, the only peaks observed are large peaks at −12.1 and −18.8 ppm. This is interpreted as slow conversion of $(\mu\text{-}H)Ru_3(\mu\text{-}COH)(CO)_{10}$ to $(\mu\text{-}H)(H)Ru_3(CO)_{11}$ at −80 °C. Warming of the sample after protonation leads to more rapid production of the dihydride species and disappearance of $(\mu\text{-}H)Ru_3(\mu\text{-}COH)(CO)_{10}$. It is this obvious correlation of warming of the sample to the rate of dihydride production which leads us to suggest that localized heating in the sample after the addition of acid to the original solution is responsible for the immediate production of the small amount of dihydride. When $[(\mu\text{-}H)Ru_3(CO)_{11}]^-$ is protonated with HSO_3F at −40 °C complete conversion to $(\mu\text{-}H)(H)Ru_3$-

(8) The second-order rate constant was estimated by defining the rate of protonation as the initial $[(\mu\text{-}H)Fe_3(CO)_{11}]^-$ concentration divided by the time took for the ^1H NMR hydride resonance to stop shifting (~3 h).

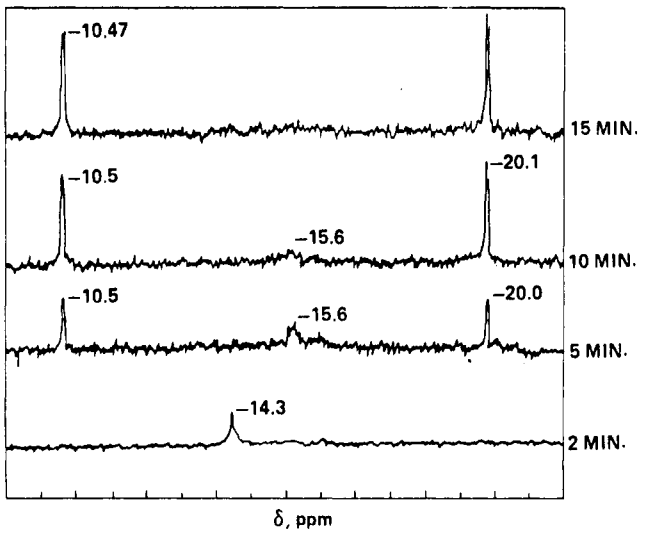

Figure 3. Time-dependent ^1H NMR spectra after addition of 1 equiv of HSO_3F to a CD_2Cl_2 solution of $[PPN][(\mu\text{-H})Os_3(CO)_{11}]$ at −80 °C. Original $[(\mu\text{-H})Os_3(CO)_{11}]^-$ hydride signal was observed at −13.6 ppm.

$(CO)_{11}$ is observed in approximately 35 min. When HSO_3F is added to $(\mu\text{-H})Ru_3(CO)_{11}^-$ at −80 °C and the sample is then warmed to −40 °C, the conversion to $(\mu\text{-H})(H)Ru_3(CO)_{11}$ is complete in approximately 1 h. As for the iron case we propose the existence of a preeqlilibrium proton exchange between $[(\mu\text{-H})Ru_3(CO)_{11}]^-$ and $(\mu\text{-H})Ru_3(\mu\text{-COH})(CO)_{10}$ to account for the broad peak that moves slowly toward the final $(\mu\text{-H})Ru_3(\mu\text{-COH})(CO)_{10}$ bridging hydride signal as more of that species is produced.

3. $[(\mu\text{-H})Os_3(CO)_{11}]^-$. The PPN salt of $[(\mu\text{-H})Os_3(CO)_{11}]^-$ which is isostructural with the Fe and Ru analogues shows a bridging hydride ^1H NMR signal at −13.6 ppm at −80 °C in CD_2Cl_2. Upon addition of 1 equiv of HSO_3F to 0.5 mL of a 0.054 M CD_2Cl_2 solution of $[PPN][(\mu\text{-H})Os_3(CO)_{11}]$ at −80 °C, the time-dependent spectra shown in Figure 3 result. A broadened peak is seen initially at −14.3 ppm, which moves upfield but rapidly vanishes as the appearance of a set of sharp doublets is seen at −10.5 and −20.1 ppm ($^2J_{HH}$ = 2 Hz) due to the terminal and bridging hydrides in $(\mu\text{-H})(H)Os_3(CO)_{11}$ which is produced very rapidly in the case of osmium. It is possible that the briefly seen broad peak initially present after acid addition is an averaging of the bridging hydride present in the original $[(\mu\text{-H})Os_3(CO)_{11}]^-$ anion with the hydride present in the intermediate $(\mu\text{-H})Os_3(\mu\text{-COH})(CO)_{10}$ species. A hydride chemical shift for $(\mu\text{-H})(\mu\text{-COH})Os_3(CO)_{10}$ is never seen as the conversion to the dihydride is comparable to the rate of protonation. From these data alone, however, we cannot exclude direct protonation at the metal, in the case of osmium, even at −80 °C.

The results discussed thus far demonstrate the reduced tendency for production of a stable oxygen-protonated species as one moves down the iron triad. It does appear that protonation first occurs at the bridging carbonyl in all three cases. In light of the work of Mays[3] and our previous work,[1,2] it was hoped that neutralizations performed with deuteriated acid would provide further information concerning the initial site and kinetics of protonation.

B. Deuterium Isotope Effects at Low Temperature. 1. $[(\mu\text{-H})Fe_3(CO)_{11}]^-$. Addition of 1 equiv of deuteriofluorosulfonic acid (DSO_3F) to 0.5 mL of a 0.068 M CD_2Cl_2 solution of $[PPN][(\mu\text{-H})Fe_3(CO)_{11}]$ at −80 °C results in the protonation of the anion and the observation of an ^1H NMR peak at −18.3 ppm after approximately 3 h. The rate of shift of the original broad −15.5 ppm peak is about the same as in the protic case (Figure 1). The +15.7 ppm peak seen in the protic case is not seen for the $(\mu\text{-H})Fe_3(\mu\text{-COD})(CO)_{10}$ species over the 5-h period of observation. The fact that no proton resonance is observed at +15.7 ppm does show that there is no scrambling between O-protonated hydrogen and the bridging hydride in the iron case at −80 °C. There is no significant kinetic isotope effect on the rate of protonation as evidenced by the fact that this rate (eq 3) is approximately the same as with protic acid (Figure 1) for the iron anion.

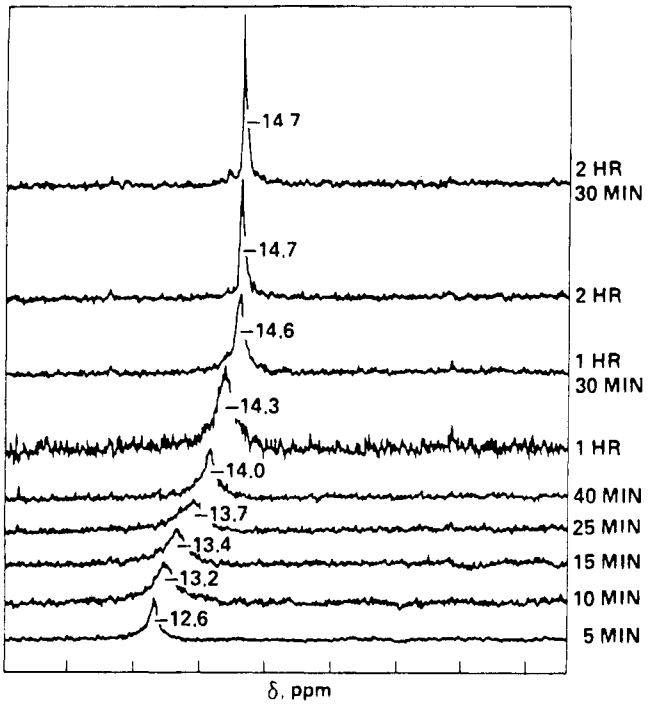

Figure 4. Time-dependent ^1H NMR spectra after addition of 1 equiv of DSO_3F to a CD_2Cl_2 solution of $[(CH_3CH_2)_4N][(\mu\text{-H})Ru_3(CO)_{11}]$ at −80 °C. Original $[HRu_3(CO)_{11}]^-$ hydride signal was observed at −13.0 ppm.

2. $[(\mu\text{-H})Ru_3(CO)_{11}]^-$. Addition of 1 equiv of DSO_3F to 0.5 mL of a 0.060 M CD_2Cl_2 solution of $[(CH_3CH_2)_4N][HRu_3(CO)_{11}]$ at −80 °C produces the time-dependent ^1H NMR spectra shown in Figure 4. Only one broad resonance is seen in the hydride region which moves slowly upfield until a sharp singlet is produced at −14.7 ppm after approximately 2.5 h. This signal corresponds to the bridging hydride present in the $(\mu\text{-H})Ru_3(\mu\text{-COD})(CO)_{10}$ produced [the slight difference in chemical shift from the −14.5 ppm peak observed in $HRu_3(\mu\text{-COH})(CO)_{10}$ may be due to an isotope effect on the chemical shift of the bridging hydride]. After 72 h at −80 °C, the ^1H NMR spectrum of $HRu_3(\mu\text{-COD})(CO)_{10}$ is unchanged, with only one resonance at −14.7 ppm and trace amounts of a dihydride species obsereved, $(H)(D)Ru_3(CO)_{11}$, with hydride resonances of equal intensity (vide infra). It can be recalled that 51 h after addition of protic acid to $[(\mu\text{-H})Ru_3(CO)_{11}]^-$ at −80 °C only the dihydride $(\mu\text{-H})(H)Ru_3(CO)_{11}$ was observed. These results indicate that after D^+ is bound to the oxygen of the bridging carbonyl, it transfers to the metal triangle at a much slower rate than a proton from the same position. In an attempt to monitor the conversion of $(\mu\text{-H})(COD)Ru_3(CO)_{10}$ to $(H)(D)Ru_3(CO)_{11}$, DSO_3F was added to $[(\mu\text{-H})Ru_3(CO)_{11}]^-$ at −80 °C and the sample then warmed to −40 °C. Here again the only signal seen initially was a sharp singlet peak at −14.7 ppm after approximately 2 h (Figure 5). However, after another 2 h

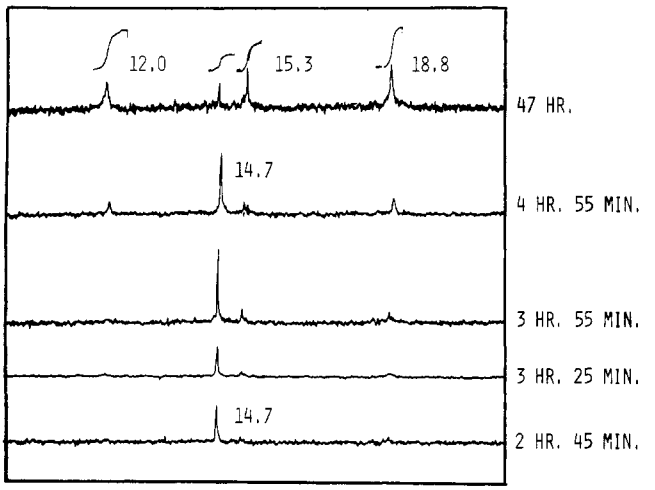

Figure 5. Time-dependent ^1H NMR spectra of $[(\mu\text{-H})Ru_3(CO)_{11}]^-$ after addition of DSO_3F at −80 °C and warming to −40 °C in CD_2Cl_2.

at −40 °C the gradual appearance of a −15.3 ppm peak simultaneously with the peaks −12.0 and −18.8 ppm $(H)(D)Ru_3(CO)_{11}$ is observed. After 47 h at −40 °C the ^1H NMR spectrum shows predominantly −12.0, −18.8, and −15.3 ppm peaks, along with a smaller amount of the −14.7 ppm $(HRu_3(\mu\text{-COD})(CO)_{10})$ peak (Figure 5). Attempts to identify the species responsible for the −15.3 ppm peak by ^{13}C NMR were unsuccessful due to the fact that the unique bridging carbonyl ligand of $[(\mu\text{-H})Ru_3(\mu\text{-CO})(CO)_{10}]^-$ could not be distinguished at −80 °C in CD_2Cl_2 either before or after addition of DSO_3F. Nine hours after DSO_3F addition to $[(\mu\text{-H})HRu_3(\mu\text{-}^{13}CO)(^{13}CO)_{10}]^-$ at −80 °C and subsequent warming to −40 °C (by which time formation of the species responsible for the ^1H NMR −15.3 ppm peak would be well underway), no identifiable ^{13}C NMR pattern is observed. An estimate of the kinetic deuterium isotope for the transfer of H^+ from the oxygen of the bridging carbonyl to the metal atoms can be made at −40 °C if one ignores the presence of the unidentified species giving rise to the hydride signal at −15.3 ppm. The first-order rate constant for the oxygen to metal hydrogen hydrogen transfer, k_H, can be estimated from the time it takes for eq 4 to go to

$$(\mu\text{-H})(\mu\text{-COH})Ru_3(CO)_{10} \xrightarrow[-40\ °C]{k_H} (H)(\mu\text{-H})Ru_3(CO)_{11} \quad (4)$$

completion as followed by ^1H NMR at −40 °C (i.e., k_H = 1 h^{-1}). The oxygen to metal deuterium transfer for $(\mu\text{-H})(\mu\text{-COD})Ru_3(CO)_{10}$ takes approximately 47 h, thus giving a $k_H/k_D \approx 47$. This value can be taken as a lower limit since conversion was not quite complete (Figure 5). These results are not surprising in light of the fact that the measurements were made 60–100 °C lower than those made by Mays.[3] The maximum isotope effect (i.e., k_H/k_D for a hypothetical symmetrical linear O–H–Ru transition state) for cleavage of the OH bond is calculated to be ~50 at −80 °C and ~25 at −40 °C using the Biegeleisen equation[4] based on expected differences in zero-point energy.[9] In order to say with certainty that these large isotope effects indicate a large tunnelling component, we must be able to determine that the activation energy difference for the protic and deuteriated cases is larger than the difference in zero-point energy between $(\mu\text{-H})(COD)Ru_3(CO)_{10}$ and $n\mu\text{-H})(COH)Ru_3(CO)_{10}$. All attempts to find several

(9) The value of k_H/k_D = 50 at −80 °C was calculated by using an infrared stretching frequency of 3600 cm^{-1} and O–D stretching frequency of 2525 cm^{-1} from the equation $k_H/k_D \approx \exp[hc/2kT(\nu_H - \nu_D)]$ (see ref 4b).

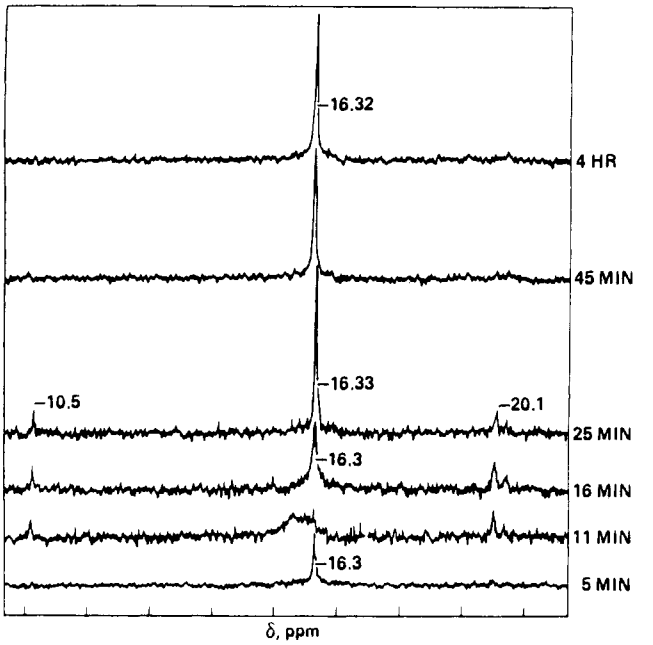

Figure 6. Time-dependent ^1H NMR spectra after addition of 1 equiv of DSO_3F to a CD_2Cl_2 solution of $[PPN][HOs_3(CO)_{11}]$ at −80 °C. Original $HOs_3(CO)_{11}^-$ hydride signal was observed at −13.6 ppm.

temperatures where the conversion from the O-protonated to the dihydride species could be observed have failed. However, these results do suggest that the isotope effects observed by Mays arise from initial formation of an O-protonated species which then rearranges to a hydrido species and where this second step is the rate-determining step in formation of the final hydride product.

3. $[(\mu\text{-H})Os_3(CO)_{11}]^-$. The addition of 1 equiv of DSO_3F to 0.5 mL of a 0.054 M CD_2Cl_2 solution of $[PPN][(\mu\text{-H})Os_3(CO)_{11}]$ at −80 °C yields the time-dependent ^1H-NMR spectra shown in Figure 6. After 4 h we observe only a peak at −16.3 ppm which we assign to the bridging hydride in $(\mu\text{-H})Os_3(\mu\text{-COD})(CO)_{10}$. The small amount of $(H)(D)Os_3(CO)_{11}$ seen initially (Figure 6) could arise from localized heat of mixing resulting in some metal deuteriation that then undergoes rearrangement to the O-deuteriated species (which may be more stable at −80 °C) or decomposition. No more $(H)(D)Os_3(CO)_{11}$ is observed even as the sample is slowly warmed from −80 to −30 °C over several hours. When compared to the neutralization with protic acid (Figure 3), a very significant deuterium isotope effect is clearly demonstrated. Here, as in the ruthenium case, the transfer of the proton from the bridging carbonyl to the metal triangle is "frozen out" by the use of D^+ in place of H^+. In order to confirm the fact that deuterium is bound to the bridging carbonyl ligand of $[(\mu\text{-H})Os_3(CO)_{11}]^-$, the neutralization with DSO_3F was conducted on ^{13}C-enriched $[(\mu\text{-H})Os_3(^{13}CO)_{11}]^-$ and the ^{13}C NMR spectrum measured. At −93 °C all of the carbonyl ligands of $[PPN][(\mu\text{-H})Os_3(^{13}CO)_{11}]$ are seen as a broad peak at 178.8 ppm in CD_2Cl_2 solution (lower temperatures are required to resolve the bridging carbonyl from the others in $[(\mu\text{-H})Os_3(CO)_{11}]^-$).[13] Approximately 2 h after addition of 1 equiv of DSO_3F one peak in the ^{13}C NMR spectrum is observed at 346.7 ppm (relative intensity = 1) as well as five sharp peaks at 179.0, 174.6, 173.0, 172.8, and 168.8 ppm (relative intensity = 4:2:1:1:2, Figure 7). This closely corresponds to the ^{13}C NMR spectrum reported by Shriver[5] for $(\mu\text{-H})Fe_3(\mu\text{-COH})(CO)_{10}$ where one downfield peak at 358.8 ppm corresponding to the μ-COH carbon and five upfield peaks (205–217 ppm) for the re-

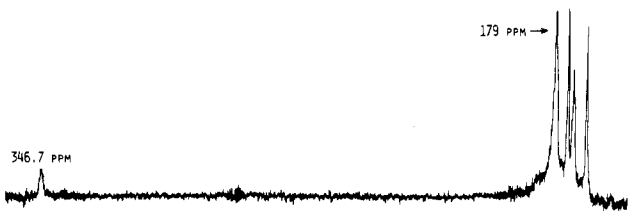

Figure 7. ^{13}C NMR spectrum of ^{13}C-enriched $[PPN][(\mu\text{-H})Os_3(CO)_{11}]$ after addition of 1 equiv of DSO_3F to a CD_2Cl_2 solution at −93 °C.

maining terminal carbonyls were observed at −100 °C. These results confirm the fact that the course of protonation for this anion is via the bridging carbonyl ligand. We also investigated the −80 °C protonation of $[(\mu\text{-D})Os_3(CO)_{11}]^-$ with HSO_3F. We observed the formation of two ^1H NMR peaks at −10.5 and −20.1 ppm of equal intensity that formed at approximately the same rate as in the protonation of $[(\mu\text{-H})Os_3(CO)_{11}]^-$ (Figure 3). The $(H)(D)Os_3(CO)_{11}$ formed has ~50% of the H in the bridging position and ~50% in the terminal position. This is consistent with the fact that the rate constant for bridge–terminal hydride exchange is 9.5×10^{-3} s^{-1} for $(\mu\text{-H})(H)Os_3(CO)_{11}$ at −80 °C ($t_{1/2}$ of 73 s).[10] This rate of exchange means that although bridge–terminal hydride exchange is slow on the NMR time scale, it is rapid relative to the overall rate of conversion of $[(\mu\text{-H})Os_3(CO)_{11}]^-$ to $(H)(D)Os_3(CO)_{11}$. Of course, we cannot exclude the possibility that a proton is transferred to the bridging position directly, with the bridging deuterium going to the terminal position. These experiments also demonstrate that placing deuterium anywhere in the cluster does not give rise to the oxygen to metal proton-transfer isotope effect described above. The same scrambling of H and D is also observed when $[(\mu\text{-D})Ru_3(CO)_{11}]^-$ is neutralized with 1 equiv of HSO_3F at −80 °C. As for the ruthenium case, we were unable to find a temperature at which smooth conversion of the O-protonated osmium species to the osmium dihydride could be observed. Finally, it should be pointed out that there is an initial broadening of averaged hydride resonance of $[(\mu\text{-H})Os_3(CO)_{11}]^-$ and $(\mu\text{-H})(\mu\text{-COH})Os_3(CO)_{10}$ which appears to be independent of the change in relative population reflected in the change in chemical shift. This is most likely due to some slow exchange with free acid in the early stages of protonation where acid concentrations are still significant. This is also seen in the ruthenium case (Figure 4). It is also possible that this early broadening results from initial protonation at a terminal carbonyl giving several protonated species in the early stages of protonation when acid concentrations are relatively high.

(10) Kiester, J. B.; Shapley, J. R. *Inorg. Chem.* **1982**, *21*, 3304.

Conclusions

The results presented here for the low-temperature protonation of $[(\mu\text{-H})M_3(CO)_{11}]^-$ anions (M = Fe, Ru, Os) demonstrate several trends: (a) the existence of preequilibrium exchange between protonated and unprotonated species after acid addition for all cases, indicating that the protonation process is not instantaneous CD_2Cl_2 at −80 °C, (b) the initial protonation at the oxygen of the bridging carbonyl in all three cases, with increased rate of formation of $(\mu\text{-H})(H)M_3(CO)_{11}$ as one moves down the triad from iron to osmium, and (c) large isotope effects are associated with the proton transfers from the bridging carbonyl to the metal core. These findings suggest that initial protonation at oxygen followed by proton transfer to the metal core may be a general process which would explain the large isotope effects observed by Mays.[3] Further investigations into the nature of proton transfer, as well as the examination of deuterium kinetic isotope effects in other types of compounds, are underway in this laboratory.

Experimental Section

Materials. The compounds $[PPN][HFe_3(CO)_{11}]$,[11] $[(CH_3CH_2)_4N][HRu_3(CO)_{11}]$,[12] and $[PPN][HOs_3(CO)_{11}]$[13] were prepared by literature procedures. Solvents ($CDCl_3$, CD_2Cl_2) were dried over molecular sieves (4A), and acids (HSO_3F, DSO_3F) were used as purchased without further purification.

Spectra. ^1H and ^{13}C NMR spectra were obtained on an IBM-NR80 spectrometer at 80 and 20.1 MHz operating in the Fourier transform mode, using liquid nitrogen to cool the sample probe for low-temperature operation.

Procedure for Low-Temperature Neutralizations. The solid compound of interest was weighed and placed into a standard 5-mm NMR tube, to which excess dry CD_2Cl_2 was added and the solution degassed with N_2 until the proper solution volume (0.5 mL) was obtained. The NMR tube, fitted with a new rubber septum, was placed into the precooled NMR probe at the desired temperature. After the solution became cold and an initial spectrum taken, the acid of interest (HSO_3F or DSO_3F) was injected directly under the solution surface by using a 5-μL syringe possessing a 15-cm needle (obtained from SGE, Inc.). For ^{13}C spectra the same procedure was employed by using 10-mm NMR tubes and 1.5–2 mL of CD_2Cl_2 solvent.

Acknowledgment. We gratefully acknowledge the National Science Foundation for support of this research (CHE-8711549).

Registry No. $[(\mu\text{-H})Fe_3(CO)_{11}]^-$, 55188-22-2; $[(\mu\text{-H})Ru_3(CO)_{11}]^-$, 60496-59-5; $[(\mu\text{-H})Os_3(CO)_{11}]^-$, 61182-07-8; HSO_3F, 7789-21-1; D_2, 7782-39-0.

(11) Hieber, H.; Brendel, G. *Z. Anorg. Allg. Chem.* **1957**, *289*, 338.
(12) Dalton, D. M.; Barnett, D. J.; Duggan, T. P.; Kiester, J. B.; Malik, P. T.; Modi, S. P.; Shaffer, M. R.; Smesko, S. A. *Organometallics* **1985**, *4*, 1854.
(13) Eady, C. R.; Johnson, B. F. G.; Lewis, J.; Malatesta, M. C. *J. Chem. Soc., Dalton Trans.* **1978**, *1358*.